Engineering Geological Characterisation of Flints

Mohammed Musa Aliyu[1], William Murphy[1], James Anthony Lawrence[2] and Richard Collier[1]

[1]Institute of Applied Geosciences, School of Earth and Environment, University of Leeds, Leeds, LS2 9JT (UK)

[2] Department of Civil and Environmental Engineering, Imperial College London, Skempton Building, London, SW7 2AZ

Abstract

The petrographic and mechanical properties of flints from the Burnham (North Landing, Yorkshire, UK), Seaford (East Sussex, UK, and Dieppe, France), and Lewes Nodular (Mesnil-Val-Plage, France) Chalk formations have been investigated. Microtexture and mineral composition of flints are studied to understand how the geological and petrophysical properties of the flint affect drilling responses to the rock and investigate any spatial variation. The flints are categorised based on physical observation: white crust; light brown; brown grey, dark-brownish-grey and grey flints. Scanning electron microscopy shows textural variation in the classes. The white crust surrounding the light brownish grey, brownish grey and grey flints from Burnham Chalk, North Landing, Yorkshire contain more calcite and have coarser more poorly cemented silica spherules by comparison to similar classes of flint from the Seaford and Lewes Formations, Anglo-Paris Basin. In these latter flints, the structure is dominated by massive quartz cement with trace calcite independent of location. Strength tests show that the grey flints from North Landing are weaker than equivalents from the Anglo-Paris Basin. It is suggested that variation in engineering properties between grey and the dark brownish grey flints is caused by mineral composition, microtexture, structure and the local/site geology of flint materials.

Keywords: Engineering; Flint; Chalk; mechanical; properties; Minerology; Microstructure

Introduction

Flint is a siliceous, cryptocrystalline rock that forms in chalk. Flint primarily composed of silica (87%-99%) with small amounts of calcite and clay minerals. Flint exists within chalk units and is found widely in Europe, parts of the USA and the Middle East. Flint has various morphologies (Fig.1): sheet; tabular; tubular; nodular; and Paramoudra (barrel shaped) flints (Bromley 1967; Clayton 1984; 1986).

The distribution of chalk in the Thames and Paris Basins means that it is often intercepted during drilling and engineering projects. Drilling is carried out for resource exploitation incuding e.g. water resources for instance in the North sea Basin (Mortimore 2012) and also during ground investigation. Engineering projects include tunnelling for infrastructure such as High speed 1 (formerly Channel Tunnel Rail Link), Crossrail 1 and the Lee Tunnel Project both in south East England. Drilling in the chalk can be affected by flints as these materials are normally extremely strong and highly abrasive, which contrasts with the very weak to weak chalk. Flints are also hard, due to their silica content, resulting in significant wear of drilling bits and the cutting heads of tunnelling boring machines (TBM). As such they present a significant construction risk and should be incorporated into risk registers associated with the geotechnical baseline report and the geological model.

Background

The mineralogical and chemical compositions of flints have received considerable attention in both archaeology and the geosciences. In archaeology, various geochemical techniques have been employed for provenance studies to constrain the origins of flint artefacts (e.g. Olausson et al. 2012; Huges et al. 2012; Prudêcio et al. 2015). For the most part these studies the colour and geochemistry of flints were used to identify their provenance.

In addition to the identification of sources, the use of flints as tools has been investigated. Pradel & Tourenq (1967) investigated the strength and hardness of Grand-Pressigny Flint with a comparison to other potential tool materials (coarse sandstone and Jasper-Opal) and noted that the Grand-Pressigny Flint was the most durable rock among the Palaeolithic geomaterials investigated. Domaǹski & Webb (2000) correlated the grain size, mineralogy and the micro fracturing and compared these parameters to the measured fracture toughness to characterise their flaking properties and found that these parameters exerted a clear control on the ability of flints to maintain a good cutting edge.

In the geosciences, X-Ray diffraction (XRD) has been used to investigate the mineralogy of flint using qualitative and quantitative approaches (e.g. Graetsch & Grunberg 2012; Jakobsen et al. 2014). Energy Dispersive X-ray Spectroscopy (EDX) (Wasilewski 2002) and Energy Dispersive X-ray Fluorescence (EDXRF) analysis (Hughes et al. 2010) have also been applied to investigate the mineralogy of flints. It was established that α-quartz is the major mineral phase in flint with minor amounts of calcite and clay minerals.

Mineralogy and geological observations

Jeans (1978) recognised that the mineral composition of flint is non-uniform noting a differentiation between the flint core and the cortex (the original outer layers). The presence of different quartz phases in various flint samples was also noted. Clayton (1984) carried out detailed microstructural studies on flints and associated crusts and provides an explanation of textural compositions and growth sequence of flints and the surrounding crust. Madsen & Stemmerik (2010) differentiated between white and dark flints and show that the dark flint possessed more massive silica cements than the white flint. Although variations in micro-structural/textural details with colour and structures of flints were investigated, the relationship between micro-structure/texture and the mechanical properties (especially the strength) of various flint morphologies (Fig. 1) from different regions remains unresolved.

The mechanical properties of flints

The variability of micro-structures/texture, chemical and mineral compositions of flint is reflected in the mechanical characteristics of flint. Iller (1963) examined the transverse rupture strength of flints and concluded that the fine grain nature of flints contributes to their strength. Since this work, a variety of different measures of the mechanical properties of flint have been investigated. These include Uniaxial Compressive Strength (UCS) (Varley 1990), tensile strength (Cumming 1999) and point load strength (Smith et al. 2003) with studies normally involving more than one test. While flints are generally considered to be extremely strong, considerable variability is observed. Cumming (1999) noted that weathered, fractured, carious (flints with network of crumbly, poorly silicified chalk) and pale flints from the White Chalk Subgroup of the Southern Province, UK, had lower strengths by comparison to other flints. Such variability was attributed to the presence of internal microfractures associated with the flint samples. These observations were supported by the work of Smith et al. (2003) who suggested that the variation in material/strength properties of flints might also depend on its geographical location which is suggestive of mineralogical or macrostructural controls.

In this paper the mineralogy and mechanical properties of flints of different morphologies from three regions are described. The relationships between flint strength, deformation properties, morphology, microtexture and colour are described with the aim of providing useful guidance for engineers and geoscientists at the desk study stage of a ground investigation. A classification of flints based on colour is proposed.

Materials and Methods

Descriptions of flint

The nomenclature for samples is as follows: the first letter relates to the formation; the second/third relates to geographic location; and the final 3 or 4th letter relates to the country. For example, flints sampled from the Burnham Chalk Formation at North Landing in the UK are given the notation B-NL-UK (BNLUK).

The test materials were from the Burnham Chalk Formation, North Landing, Yorkshire, UK (BNLUK) [TA 243 706], the Seaford Chalk Formation, East Sussex, UK (SESUK) [TA 675 510] and at Dieppe, France (SDFr) [TW 196 769], and the Lewes Chalk Formation at Mesnil-Val-Plage, France (LMFr) [TW 539 265] (Fig. 2). Samples were collected from sea-cliff exposures and occasionally, from fresh rock falls where the stratigraphy could be identified. In the latter case, samples were only collected where flints were still surrounded with thick chalk deposits that were assumed to protect the flint from impact damage. Some of the flint blocks from the different sites are shown in Fig. 3 and description of flint samples are provided below.

Flints from the Burnham Chalk North Landing, Yorkshire, United Kingdom.

The flint samples from the North Landing, UK are tabular, mostly grey (Figs. 3a and b) and highly fractured (Fig. 3c, both macro/microfractures). Fracturing in these samples might be associated with tectonic activity as the collection site is near the Flamborough Head faults. The white crust (Fig. 3a) which is commonly 20 mm thick and is stronger than the surrounding chalk, but weaker than the enclosed flint core. These flint samples have higher calcite content than other flints. Most of these flint samples are up to 300 mm thick and comprised of significant quantity of partially silicified carbonate inclusions (Fig. 3b) and in some cases most of the sample is dominated by the light grey flint. Brownish grey flints are also found in the North Landing Chalk with significant quantity of calcite inclusions too (Fig. 3b).

Flints from the Anglo-Paris Basin, United Kingdom and France.

The flints in the Anglo-Paris Basin chalk are shown in Fig. 3d-f. Fig. 3d is a flint from the Seaford Chalk, East Sussex, UK, Fig. 3e is a flint in the Seaford Chalk, Dieppe, France and Fig. 3f is flint in the Lewes Chalk, Mesnil-Val, France. These flint samples are mostly dark brownish grey, with a few silicified inclusions. These inclusions appear as light brownish grey irregular shaped zones in the samples. The dark brownish grey flints appeared more competent than the grey flints. Microfractures are rarely seen in these flints, and the white crust surrounding the dark brownish grey flints are thinner and harder when compared with those surrounding the grey flints from the Burnham Chalk Formation.

Geology of the Study Sites

The geology at North Landing is described in Mortimore et al. (2001). The Burnham Chalk Formation (Turonian-Santonian, Fig. 4) includes the entire Sternotaxis plana zone to the lower part of the Micraster cortestudinarium zone. The Formation overlies the Welton Chalk Formation and is overlain by the Flamborough Chalk Formation. It is characterised by the tabular flints (≥ 0.3m thick) (Wood & Smith 1978; Gale & Rutter 2006), Paramoudra and semi-tabular flints. It comprises thinly bedded chalk with flints and is 130-150 m thick in this area (Mortimore et. al. 2001; Hopson 2005). The base of this formation has more flint bands than other parts of the formation (see Wood & Smith 1978) and is characterised by conspicuous layers of light grey, highly fractured carious tabular flints.

The geology of the chalk at the sites sampled in the Anglo-Paris basin is described by Bristow et al. (1997) and Mortimore et al. (2001). The Seaford Chalk Formation (middle Coniacian-middle Santonian, Fig. 4) is described in Mortimore (1986); Mortimore & Pomerol (1997); Bristow et al. (1997) and Mortimore et al. (2001).The formation is composed of pure (>98%) calcium carbonate, very weak, white, fine-grained chalk, with extensive bands of dark nodular flints, and sheet flints at the type locality. The formation is bound at the top by marl seams and by the basal marker the Shoreham Marl. The formation also includes of the Seven Sisters Flint which is a conspicuous marker bed and is also traceable along the French coast (Upper-Normandy and Picardy) (Mortimore et al. 1986).

At the sampling site at Mesnil-Val in Picardy, France, the dominant chalk formation is the Lewes Nodular Chalk Formation (Upper Turonian-Lower Coniacian stage, see Fig. 4) as described in Mortimore (2001). The Lewes Chalk Formation comprises marl seams, and well bedded, nodular chalk with nodular flint bands. These flint bands are parallel to the bedding, laterally extensive and traceable in the stratigraphy (Mortimore 1986; Mortimore &

Pomerol 1987; Senfaute et al. 2009). Apart from nodular flint bands, tubular and semi-tabular flints are also present in places in the chalk cliffs.

Sample description

The flint samples are initially classified on the basis of the geological features, mainly body colour characteristics (Figs. 3a-f and 5). The flint colour classification is based on Munsell colour chart as given in Table 1. The frequently used notations representing flint types, geological units and geographical locations are provided in Table 2. Flint samples were tested at their natural moisture content and at laboratory temperature. The method/specifications (Table 3) and typical sample sizes/geometries (Table 4) used for the geomechanical tests are 25, 12, 22, 25, and 25 mm, for UCS, To, $I_{s(50)}$, E_s, and ν_s respectively.

Microstructure and mineralogical Characterisation

The external morphology, grain shape, orientation and degree of crystallisation/cementation of the flint are characterised using scanning electron microscopy (SEM) to aid in explaining the physical and mechanical properties of flints. The mineralogy, including the silica phases, is assessed using X-ray diffraction (XRD).

Scanning Electron Microscope

SEM analysis, including secondary electron images (SEI) was conducted on samples with size of approximately 10 x 10 x 5 mm. The analysis was conducted on twelve flint samples selected to be representative of the various flint classes (Fig.5). These were coated with gold in a BIO-RAD-SC500 Sputter coater for 4 – 5 minutes to inhibit the concentration of electrical charge on the samples. The coated samples were analysed using a JEOL-JSM-6610LV SEM machine equipped with an Oxford Instrument Energy Dispersive X-rays (EDX) detection analyser, which is used to identify and quantify mineral phases of the samples. Images were captured using an accelerating voltage of 15 keV.

X-Ray Diffraction

XRD analysis was also performed on flint specimens similar to those characterised using the SEM. The analysis was carried out using a D8 diffractometer. Flint samples were ground into powder and pressed into a mount in order to produce a randomly oriented powder. The mounts were analysed in turn. A Cu kα radiation source was used. The specimens were scanned over an angular range of 2-90^o 2θ, with a step size of 0.01^o. The data were processed using Bruker EVA search match software for phase identification while

Bruker TOPAS profile and structure analysis software were used to quantify the mineral phases present.

Geomechanical Properties Tests

The methods used for testing samples are outlined in Table 3 and the geometry of tested samples reported in Table 4. The majority of these methods use standard test procedures. Deviations from the standard method discussed. Two testing machines were used. These were the MAND Universal Compression Testing machine (250 kN capacity with a precision 0.1 kN) for the tensile test and the Denison compression machine (capacity of 2000 kN with precision of 0.05 kN) for compression testing.

Bulk density ($\boldsymbol{\rho}$)

The bulk density ($\boldsymbol{\rho}$) of flint was determined using the caliper method. The bulk mass of each specimen was measured using a digital scale. The bulk volume was obtained from the mean of five readings for each dimension taken at various points of the specimens. Bulk density was calculated from the relationship between the bulk mass and the bulk volume of each flint specimen (Equation 1).

$$\rho = \frac{bulk\ mass\ (M_b)}{bulk\ volume\ (v_b)} \qquad (1)$$

Where: ρ is the bulk dendity (Mg m^{-3})

Tensile strength (T_o)

For the tensile strength (T_o), the Three-point beam method described by Brook (1993) was used to determine the tensile strength of flint by bending. The test was developed to estimate tensile strength by subjecting samples to stress by applying steady central load between two ball bearings until the samples fail by bending. The positioning of the bearings is dictated by sample length. The concentrated load applied to the sample causes tensile deformation along the point of the applied load, which leads to a tensile failure.

The Three-point beam method was used instead of the direct tensile test and the Brazil test because:

1) Less sample preparation and a surface finish was required and no surface finish was required;

2) Smooth or flat ends were not required

These requirements mean that a beam of flint can be more easily prepared and tested using this method than the standard disc required for the Brazil test or the direct tensile test. The tensile strength derived from beam method was found to compare well with that of direct pull test (Brook 1993) and with tensile strength obtained from the Brazilian test for flint (Cumming 1999). The three-point-beam test was carried out using the MAND universal compression testing machine. Tensile strength was calculated using Equations 2 & 3.

$$T_0 = \frac{P}{G} \qquad (2)$$

$$G = \frac{4bd^2}{3l} \qquad (3)$$

Where: To is the tensile strength (MPa), P is the failure load (kN), G is the geometry factor, b is the breadth of the sample (mm), d is the thickness of the sample (mm), l is the span between the ball bearings.

Point Load Strength Test

Point load strength index ($I_{s(50)}$) of flint was measured using an ELE point load tester with a loading capacity of 56 kN and a precision of 0.05 N. Both blocks and irregular specimens were tested in accordance with ISRM (2007) suggested methods. The dimensions of the specimens range (L=25-90 mm), (W=19-45 mm), and (D=15- 44 mm). Sample geometry was constrained by challenges of preparing flint samples. The samples sizes used were within the 50±35 mm tolerances contained in the suggested method. Samples were tested at a loading rate resulting in failure between 10-60 seconds after the start of the test. The failure loads were then recorded,the $I_{s(50)}$ for each specimen was calculated using Equations 4 to 9 (ISRM 2007).

$$A = W \times D \qquad (4)$$

$$De^2 = \frac{4D}{\pi} \qquad (5)$$

$$De = \sqrt{De^2} \qquad (6)$$

$$I_s = \frac{(P \times 1000)}{De^2} \qquad (7)$$

$$F = \left(\frac{De}{50}\right)^{0.45} \qquad (8)$$

$$I_{s50} = F \times I_s \qquad (9)$$

Where: A is the minimum cross sectional area of the point of contact for the loading platens on the sample (mm^2), De is the equivalent sample diameter (mm), F is the Size correction factor, I_s the Uncorrected Point load strength index (MPa), and $I_{s(50)}$ is the corrected Point load strength index (MPa).

Uniaxial Compressive Strength (UCS) Test

Uniaxial compressive strength (UCS) of flint was measured using Denison machine with the capacity of 2000 kN at loading rate of 0.5 $MPas^{-1}$. The machine has an accuracy of 0.05 kN. The test was conducted on both cores and cuboid flint specimens in accordance with ASTM D2845 2000; ISRM 2007; ASTM D7012-07 2010 suggested methods. The typical sample diameter of 25 mm was used. The choice of these sizes was informed by the repeated failure of attempts to produce cylindrical core samples of NX size (54 mm). The cuboid flint specimens were only prepared for the flint samples from the Burnham Chalk Formation due to difficulty in preparing cylindrical samples because of fractures/joints and carbonate inclusions in the samples.

Young's modulus and Poisson's ratio

The deformability (Young's modulus and Poisson's ratio) of flint specimens was determined in accordance to ISRM 2007 suggested methods from the strain measurements. Strain was measured using 5 mm electrical resistance strain gauges. The axial stresses, axial, and lateral strains, were recorded using a windmill logger. These data were used to plot stress-strain curves from which elastic properties comprising static Young's modulus (E_s), and static Poisson's ratio (ν_s) were determined. The average method was used to determine the E_s of flint using Equation 10. This involves deriving E_s from the approximate linear part of the axial stress-strain curve (ISRM 2007). The ν_s was then calculated from the relationship between E_s and the slope of diametric stress-strain curve using Equation 11.

The deformability of all the investigated flint specimens was measured except the flint specimens from the Burnham Chalk Formation. The deformability of these specimens was not measured because the strain gauges detached from the specimens at early stage of loading due to spalling of flints under load. Spalling of chips of these flints was likely associated with closely spaced (c. 10 – 15 mm) orthogonal incipient fractures in the specimens.

$$E_s = \frac{\Delta\ Axial\ stress}{\Delta\ Axial\ strain} \quad (10)$$

$$v_s = \frac{E_s}{Slope\ of\ diametral\ curve} \quad (11)$$

.

The physical and mechanical properties were statistically analyse using One-way ANOVA and Post-Hoc tests using Tukey's test as described in Stevens (2007). The One-way ANOVA was used because the normality test using Shapiro-Wilk shows most of the data was drawn from normally distributed population (Table 5) except in four cases where normality was rejected (bold in Table 5). In the four cases, two have about 50 specimens in which case normality can be assumed due to large sample size in the population. The two remaining cases E_s for SDFr and To for LMFr (both in Table 5) were treated as non-normally distributed data. Thus, to check the influence of distributions of data, both parametric and non-parametric statistics were used to analyse the overall results (summarised in Tables 6 & 7).

Results

Petrographic Observations

The principal minerals identified in all the flint samples investigated were α-quartz and calcite, the percentages of which vary with flint structure and geographic locations (Table 5). A summary of the mineralogy of different flint structures and class by location is given in Table 8. Table 9 describes the micro morphological observation from the different flint classes.

In the white crusts of the Burnham Chalk Formation, granular, flaky calcite crystals with clusters of quartz microspheres and traces of cryptocrystalline quartz are evident (BNLUK, Fig. 6a). The white crust of the Seaford Chalk from both sites have homogeneous phase dominated by cryptocrystalline quartz (Figs. 6a-c). The recrystallisation of quartz grains into massive quartz cements is apparent in the white crust (WCr) of the Seaford Chalk Formation

Dieppe, France (Fig. 6c). The WCr from both Seaford Chalk formations are relatively more cemented than those from BNLUK and have amorphous silica particles (enclosed in white in Figs 6b & c) with some clusters of quartz microspherules (indicated by the arrows in Fig. 6c).

Spherical quartz grains that have transformed into clusters of quartz microspheres are seen in the light brown grey, brown grey and grey flints of the Burnham Chalk (Figs. 6d, h, and l). Quartz cements also occur intermittently in these samples and are also observed in the light brownish grey flints (Figs. e-g). The clusters of quartz microspheres are more pronounced in the GF (Fig. 6l) from the Burnham Chalk Formation, North Landing, UK (BNLUK) than light brownish grey flints from the same chalk formation. Spherical quartz grains with interparticle pores and microfractures are seen in the LBG of the BNLUK samples (dark arrows in Fig. 6d). These interparticle microfractures are also evident in the BG flint of the BNLUK category.

The LBG and DBG flints in the Seaford Chalk at East Sussex, (SESUK), Seaford Chalk at Dieppe, France (SDFr) and Lewes Chalk at Mesnil-Val, France, (LMFr) appeared distinct (Figs. 6i-k). These flint samples exhibit networks of massive quartz cements formed by the agglomeration of quartz grains (shown by the gradation between quartz grains/flakes and cements in Fig. 6k). These flint types show greater cementation compared to those of GF (BNLUK).

Mechanical Properties by Location

The results of the mechanical properties of flints are expressed as box and whisker plots (Fig. 7a-f).. The main statistical analysis of the results is given in Tables 6 and 7 presented according to locations and geological units which vary with flint class. Box and Whiskers are used to show the overall distribution of the results. Cross plots are used to show the strength-density relationship of flint (Fig. 8), the influence of sample sizes on strength of flints and the distribution of some engineering geological parameters (Fig. 9 a & b).

Figs.7a – d show data for the flints obtained from North Landing and Anglo-Paris basins. It can be seen that by comparison to flints from the south of England and France, those from North Landing are significantly less dense (mean density 2.42 Mgm^{-3} as opposed to 2.66-2.69 Mgm^{-3}). This tends to suggest a lower degree of silicification (Fig. 6a) than in the flints found within the southern Province chalk. Concurrently, it is therefore unsurprising that To, UCS and $Is_{(50)}$ for the North Landing flints are significantly lower than those from elsewhere. In Figs 7b, c and d, it is clear that the flints from the Anglo-Paris basis (from the Seaford and Lewes Chalk formations) show a range of mechanical properties which are broadly similar. Equally, as can be seen in 7e and 7f, Young's Modulus and Poisson's Ratio for flint samples extracted from the English and French sites are broadly similar.

While it can be seen that there is some overlap in the natural material variation, the overlap is small (Tables 6 & 7).

Tensile Strength (T_o)

Fig.7b shows results of variations in tensile strength (T_o) as summarised in Tables 6-7. Flints in the Burnham Chalk Formation, North (BNLUK) generally showed lowest mean (Table 6) and ranges of tensile strength (Fig. 7b) compared with those of Seaford and Lewes Chalk formations. In some specimens of the BNLUK flints a weak correlation between tensile strength and carbonate content was observed. This correlation is indicated by the absence of the two major data point clusters (observed in Figs. 7c & d) exhibiting differences in strength between samples with higher calcite inclusions and samples with lower calcite inclusions. The T_o values for samples from the Seaford and Lewes Chalk formations were all greater than those for the Burnham Chalk Formation and were similar (in both the mean and median values, Table 6).

Point Load Strength Index ($I_{s(50)}$)

A similar pattern to that seen during the tensile testing program was observed during the point load strength index testing. The plot of $I_{s(50)}$ for the four flint types is in Fig. 7c. $I_{s(50)}$ values for flints from the Burnham Chalk are distinctly lower than those from other locations. The recorded values of $I_{s(50)}$ were in the range of 3.07-12.31 MPa flint in the Burnham Chalk Formation, North (BNLUK). A comparison of the $I_{s(50)}$ values between dark brownish grey flints in the Seaford Chalk Formation at East Sussex, UK, Dieppe, France and flints in the Lewes Chalk Formation does not show any significant differences (Tables 6 & 7).

Uniaxial Compressive Strength

The UCS of the flints studied is shown in Fig. 7d and the statistical observations are presented in Tables 6-7. It should be noted that in both statistical approaches employed, grey flints in the Burnham Chalk, North Landing (BNLUK) consistently remain the weakest material as against the dark brownish grey flints from other formations. This is consistent with the trends in T_o and $I_{s(50)}$ results. The UCS of flints in the Seaford Chalk Formation at East Sussex, Dieppe, France and for flints in the Lewes Chalk Formation corresponds to the extremely strong category. However, a significant difference exists in the UCS of the flints from Burnham Chalk Formation forming two major clusters with mean UCS and standard deviation as low as 112.2±71.0 MPa within a range of 25.2 to 232.4 MPa were recorded. The wide range observed in these samples is associated with calcite inclusions and microfracturing in the samples.

The deformation characteristics of flints, elastic properties comprising Young's modulus (E_s), and static Poisson's ratio (ν_s) were determined (Figs. 7e and f) and Tables 7-8 provide the summary of the overall results. The E_s ranges, mean and standard deviation values for flints in the Seaford Chalk Formation from East Sussex and from Dieppe and flints in the Lewes Chalk Formation indicate these flints are extremely stiff, with very slight variation in stiffness among the samples (Tables 6 & 7). As observed in all the mechanical tests, the ν_s for the dark brownish grey flints from the Seaford and Lewes Chalk formations representing the three respective sites were similar (Fig. 7f and summarised in Tables 6 & 7). These ν_s values range from 0.050-0.181 and the overall data points reflected the heterogeneity within the individual flint specimens characterised by the presence of partially silicified inclusions and minor variations in mineral composition.

Discussion

General observations

Due to the different tectonic setting of each site an investigation into the effect this has on the geomechanical properties of flint was possible.

The results of physical and mechanical investigations (summarised in Tables 6 & 7) indicate that the engineering properties of flints vary with flint class. The relationship between ρ and UCS is presented in Fig. 8 The effects of sample sizes on the overall strength results assessed from the cross plots of strength and sample sizes (Figs 9a & b). Figs. 9a & b suggest that variations in sample sizes do not affect the present findings as there was no observed clear relationship in the cross plots.

The results from the mechanical tests show considerable variation in flint strengths which is consistent with other studies (e.g. Cumming 1999; Mortimore et al. 2011; Smith et al. 2003).

If flints are classified into dark brown-grey flints (DBG) and grey flints (GF), it is generally observed that the densest, strongest and stiffest materials fall into the DBG category. This is consistent with the mineralogical observations as the DBG category has lower calcite content, but higher quartz content when compared with GF with lower quartz content and higher calcite content (Table 8).

The Burnham Conundrum

Even at the stage of sample preparation and field observation it was apparent that the flints drawn from the Burnham Chalk at Flamborough Head were significantly different from those observed in the chalk of the Anglo-Paris basin. This difference is characterised by the presence of centimetre scale fractures in the flint (Fig. 1a). These tend to form in a bedding-parallel orientation and at 90º to bedding. This has led to two possibilities: (i) the flints in the Burnham Chalk are fractured or (ii) the flints at Flamborough Head are fractured. The higher calcite content observed could explain the strength properties of these flints, but not only the presence of the fracturing. These flints showed less cement and possessed larger, more spherical quartz grains compared with other flints (see SEM images Figs. 6a-l).

Grey flints from the Burnham Chalk Formation were collected in Lincolnshire (mean UCS=310 MPa, mean ρ=2.49 Mgm^{-3}). These materials do not contain similar centimetre scale fractures and it is suggested that the proximity to extensional structures of the North Sea Basin has resulted in the flexure of the Chalk. In the Chalk itself, this is readily accommodated via layer parallel slip, whereas for the more brittle flints fracturing is the only available mechanical option. This tends to confirm the postulated effects of tectonics on the strength of flints from the Southern Province of the UK suggested by Cumming (1999). It seems likely that this is an effect associated with extensional tectonism rather than compressional since the extremely high compressive strengths of flint are unlikely to allow brittle compression fracture to develop.

Mineralogical controls on mechanical properties.

The mineralogical control on the mechanical properties of flint is the percentage of silica within the sample. The colours of flints generally reflect of the silica-calcite ratios within the rock. Although some halite was observed on XRD traces, this is contamination from sea spray. Generally there is an increase in the quartz content from the white crust through the light brown grey; brownish grey; grey flint and into the dark brown grey flints (Table 8). There is conversely an increase in the carbonate content.

The evidence of high sphericity of quartz grains and interparticle voids in the weaker, less dense grey flints compared to the stronger, denser, intensely silicified micro fabrics of the dark brownish grey flint supports the hypothesis that the microtexture and the microstructure of flint exert significant control on the engineering behaviour of flint (Tables 6-8). Fig.8 shows that the highly cemented/silicified dark brownish grey flints showed significantly higher strength and density than the predominantly grey flints. There is some natural scatter which is a function of natural variability of the flint materials.

Reported values of Young's modulus show small variations from previously reported observations (see Table 10, Pabst & Gregorová 2013). However, it is likely that such variations fall within the range of uncertainty of natural materials and can be attributed to observational bias due to different techniques being used in the measurement. Similarly, measured Poisson's ratio (ν_s) of flint samples from the Seaford Chalk and Lewes Chalk formations are broadly consistent with the results of Gercek (2007).

Summary and Conclusions

An investigation of three groups of flints from the United Kingdom and France is reported. Significant differences in the mechanical properties of flints exist.

The principle control on the mechanical properties of flint is the relative proportions of quartz to calcite in the rock. Such proportions also control the colour of the materials and therefore it is possible to classify flints on the basis of colour. The colour ranges from the white crust (often found around flints), which is in effect a highly silicified chalk, through to the dark brown grey flints with the lowest percentage of calcium carbonate. Given the empirical relationship between abrasivity and quartz content colour may be a useful predictor of potential abrasivity at the desk study stage approach of a site investigation. Further investigation is required to confirm the validity of this relationship outside the Anglo-Paris basin.

It is observed that the flints found in the Burnham Chalk Formation from North Landing in Yorkshire show lower densities and lower strength properties than other materials. The dark brownish grey flints in the Seaford and Lewes Formations have similar strength values supporting the view that colour is a useful predictor regardless of geographic location and stratigraphic control. The fracturing in the flints found at North Landing is likely to be a tectonic effect and the potential for such fracturing should be considered during site investigations in the proximity of large extensional faults

Acknowledgement

This research project is funded through a doctoral training award from the Petroleum Technology Development Fund (PTDF), Nigeria. The American Association of Petroleum

Geologists is acknowledged for supporting part of the French fieldwork. Mr Kirk Handley and Dr John Martin are acknowledged for assistance in geotechnical testing. Dr. Algy Kazlauciunas and Lesley Neve assisted with SEM and XRD analyses respectively. The encouragement and advice of two anonymous reviewers is gratefully acknowledged.

References

ASTM 2000. Standard test method for laboratory determination of pulse velocities and ultrasonic elastic constants of rock (D2845-00). West Conshohocken, American Society for Testing Materials, ASTM.

ASTM 2010. Standard test method for compressive strength and elastic moduli of intact rock core specimens under varying states of stress and temperatures (D7012). Philadelphia, American Society for testing materials, ASTM.

BRISTOW, C. R., MORTIMORE, R. N., & WOOD, C.J. 1997. Lithostratigraphy for mapping the Chalk of southern England. Proceedings of the Geologists' Association, **108** (4), 293-315.

BROCH, E., & FRANKLIN, J. A. 1972. The point-load strength test. International Journal of Rock Mechanics and Mining Sciences & Geomechanics. **9** (6), 669-676. Pergamon.

BROMLEY, R. G. 1967. Some observations on burrows of Thalassinoidean Crustacea in chalk hardgrounds. Quarterly Journal of the Geological Society, **123**, 157- 177.

BROMLEY, R. G., SCHULZ, M. G., & PEAKE, N. B. 1975. Paramoudras: giant flints, long burrows and the early diagenesis of chalks. Kongelige Danske Videnskabernes Selskab Biologiske Skrifter (Biological Series), **20** (10), 31.

BROOK, N. 1993. The measurement and estimation of basic rock strength. Comprehensive rock engineering, **3**, 41-66.

CLAYTON, C. J. 1986. The chemical environment of flint formation in Upper Cretaceous chalks. In: SIEVEING, DE G. & HART, M. B. (eds) The scientific study of flint and chert. Cambridge University Press**,** Cambridge, 43-53.

CLAYTON, C. J. 1984. The geochemistry of chert formation in Upper Cretaceous chalks. Unpublished PhD Thesis, King's College London (University of London).

CUMMING, F. M. D. F. 1999. Machine tunnelling in chalk with flint with particular reference to the mechanical properties of flint. Unpublished PhD Thesis, University of Brighton.

DOMAŃSKI, M., & WEBB, J. A. 2000. Flaking properties, petrology and use of Polish flint. Antiquity, **74** (286), 822-832.

GALE, I. N., & RUTTER, H. K. 2006. The chalk aquifer of Yorkshire: Keyworth: British Geological Survey. Research Report, RR/06/04, 1-62.

GERCEK, H. 2007. Poisson's ratio values for rocks. International Journal of Rock Mechanics and Mining Sciences, **44** (1), 1-13.

GRAETSCH, H. A., & GRÜNBERG, J. M. 2012. Microstructure of flint and other chert raw materials. Archaeometry, **54** (1), 18–36.

HOPSON, P. 2005. A stratigraphical framework for the Upper Cretaceous Chalk of England and Scotland with statements on the Chalk of Northern Ireland and the UK Offshore Sector. British Geological Survey Research Report No. RR/05/01.

HUGHES, R. E. , HÖGBERG, A., & OLAUSSON, D. 2012. The Chemical Composition of Some Archaeologically Significant Flint from Denmark and Sweden. Archaeometry, **54** (5), 779-795.

HUGHES, R. E., HÖGBERG, A., & OLAUSSON, D. 2010. Sourcing flint from Sweden and Denmark. Journal of Nordic Archaeological Science, **17**, 15-25.

ILER, R. K. 1963. Strength and structure of flint: Nature, **4900**, 1278-1279.

ISRM, 2007. The complete ISRM suggested methods for rock characterization, testing and monitoring: 1974-2006: In Ulusay, R., & Hudson, J. A. (eds) Suggested methods prepared by the commission on testing methods, International Society for Rock Mechanics, Commission on Testing Methods (ISRM Turkish National Group).

JAKOBSEN, F., LINDGREEN, H., & NYTOFT, H. 2014. Oil-impregnated flint in Danian Chalk in the Tyra Field, North Sea Central Graben. Journal of Petroleum Geology, **37** (1), 43-53.

JEANS, C. V. 1978. Silicifications and associated clay assemblages in the Cretaceous marine sediments of southern England. Clay Minerals, **13** (1), 101-126.

MADSEN, H. B., STEMMERIK, L., & SURLYK, F. 2010. Diagenesis of silica-rich mound-bedded chalk, the Coniacian Arnager Limestone, Denmark. Sedimentary Geology, **223** (1-2), 51–60.

MORTIMORE, R. N. 1986. Stratigraphy of the Upper Cretaceous White Chalk of Sussex. Proceedings of the Geologists' Association, **97** (2), 97-139.

MORTIMORE, R. N. 2011. A chalk revolution: what have we done to the Chalk of England? Proceedings of the Geologists' Association, **122** (2), 232-297.

MORTIMORE, R. N., NEWMAN, T., ROYSE, K., SCHOLES, H., & LAWRENCE, U. 2011. Chalk: its stratigraphy, structure and engineering geology in east London and the Thames Gateway. Quarterly Journal of Engineering Geology and Hydrogeology, **44** (4), 419-444.

MORTIMORE, R. N., & POMEROL, B. 1997. Upper Cretaceous tectonic phases and end Cretaceous inversion in the Chalk of the Anglo-Paris Basin. Proceedings of the Geologists' Association, **108** (3), 231-255.

MORTIMORE, R. N., WOOD, C.J., & GALLOIS, R. W. 2001. British upper Cretaceous stratigraphy, Geological Conservation Review Series, No. 23, Joint Nature Conservation Committee, Peterborough, 558 pp.

OLAUSSON, D., HUGHES, R. E., & HÖGBERG, A. 2012. Provenance studies on Scandinavian Flint. Acta Archaeologica, **83** (1), 83-86.

PABST, W., & GREGOROVÁ, E. 2013. Elastic properties of silica polymorphs–a review Ceramics-Silikaty, 57, 167.

PRADEL, L., & TOURENQ, C. 1967. Les matériaux de Fontmaure Choix des Paléolithiques et measures des caractères physiques. Bulletin de la Société préhistorique française. Comptes rendus des séances mensuelles, LXXXI-LXXXV.

PRADEL, L., & TOURENQ, C. 1972. Choix des matériaux par les Paléolithiques de Fontmaure et essais de fragmentation dynamique. Bulletin de la Société préhistorique française. Comptes rendus des séances mensuelles, **69** (1), 12-12.

PRUDÊNCIO, M. I., ROLDÁN, C., DIAS, M. I., MARQUES, R., EIXEA, A., & VILLAVERDE, V. 2015. A micro-invasive approach using INAA for new insights into Palaeolithic flint archaeological artefacts. Journal of Radioanalytical and Nuclear Chemistry, **308**, 1-9.

SENFAUTE, G., DUPERRET, A., & LAWRENCE, J. A. 2009. Micro-seismic precursory cracks prior to rock-fall on coastal chalk cliffs: a case study at Mesnil-Val, Normandie, NW France. Natural Hazards and Earth System Science, **9** (5), 1625-1641.

SMITH, N. A., HISLAM, J. L., & FOWELL, R. J. 2003. A Note On the Strength of Flint Particles. In: Handley, M. & Stacey, R. Technology roadmap for rock mechanics. South African Institute of Mining and Metallurgy, **2**, 1105-1108.

STEVENS J. P. 2007. Intermediate Statistics A Modern Approach. Lawrence Erlbaum Associates, London.

VARLEY, P.M. 1990. Machine excavation of chalk rock at the first South Killingholme gas cavern, South Humberside. In: Burland, J.B., Mortimore, R.N., Roberts, L.D., Jones, D.L. & Corbett, B.O. (eds) Chalk. Proceedings of the International Chalk Symposium, Brighton Polytechnic, 1989. Thomas Telford, London, 485–492.

WASILEWSKI, M. 2002. Mineralogical investigation of desert patina on flint artifacts: A case study. Mediterranean Archaeology and Archaeometry, **2** (2), 23-34.

WOOD, C. J., & SMITH, E. G. 1978. Lithostratigraphical classification of the chalk in North Yorkshire, Humberside and Lincolnshire. Proceedings of the Yorkshire Geological Society, **42**, 263-287.

FIGURE CAPTIONS

Fig. 1:(a) Tabular Flint in Burnham Chalk Formation, North Landing, UK ; (b) Tubular Flint, Lewes Chalk Formation, France; (c) Paramoudra Flint, Burnham Chalk Formation, Ucerby Vale Quarry, Lincolnshire, UK; (d) Nodular Flint, Seaford Chalk Formation, East UK; Sussex, (e) Sheet Flint, Seaford Chalk Formation, East Sussex, UK.

Fig. 2: Study locations.

Fig. 3: (a-f) Flint Blocks from the four (4) study sites showing different structures and colours of flint. (a-c) Represent flint blocks from the North Landing, UK. Note the white crust in (a), brownish grey flint with white inclusions in (b), and highly fractured grey flint in (c). (d, e and f) Dark brown flint from Seaford Chalk, UK, France and Lewes Chalk, France respectively. Note the presence of light brownish spots on all the dark brown flints.

Figure. 4: Simplified Stratigraphy of the Upper Cretaceous Chalk in the study sites (Adapted from Bristow et al., 1997; Mortimore et al. 2001; Mortimore 2011; Duperett et al. 2012).

Figure 5: Different flint structures and colours used for petrographic analysis.

Figure 6: SEM images flint samples showing different morphologies. (a), (b),and (c) WCr from BNLUK, SESUK, and SDFr respectively (CC is Calcite crystals). (d), (e), (f) and (g) LBG from BNLUK, SESUK, SDFr, and LMFr respectively. (h) BG from BNLUK showing microfractures, and equigranular microspheres forming clusters. (i), (j), and (k) DBG respectively from SESUK, SDFr, and LMFr revealing dense and massive quartz cements. (l) Grey Flint (GF) from BNLUK indicating spherical quartz grains similar to (h) but appeared more cemented.

Figure 7: (a) Density of flints (Mgm^{-3}); (b) Tensile strength (MPa); (c) Point load strength index (MPa) ; (d) UCS (MPa); (e) Static Young's Modulus (GPa); (f) Static Poisson's ratio of flints from all the study sites.

Figure 8: UCS against density of flints.

Figure 9: Sizes of samples against (a) UCS, (b) $Is_{(50)}$ of flints.

Figure 10: Tensile strength of flint against sizes of flint samples.

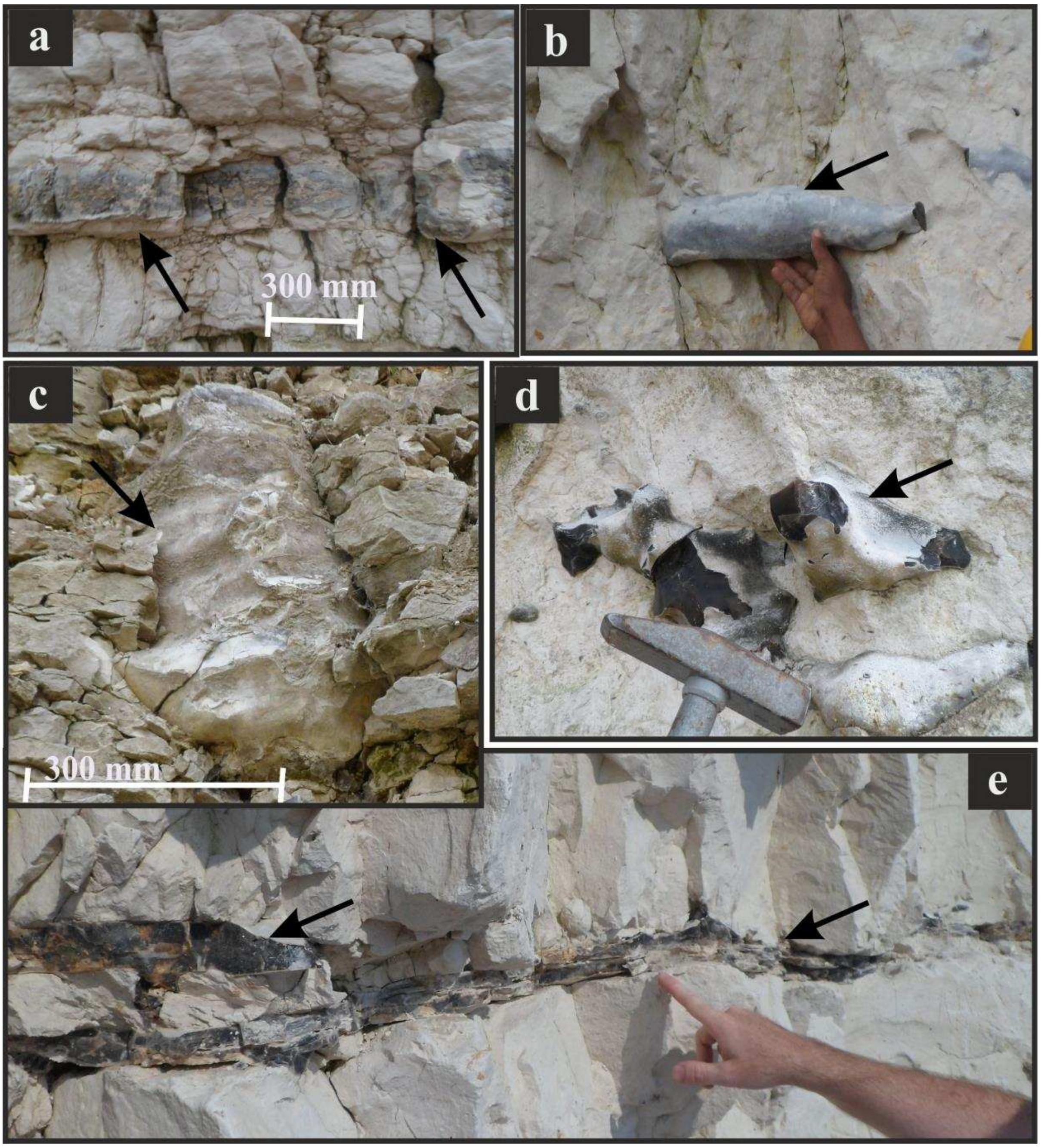

Fig. 1

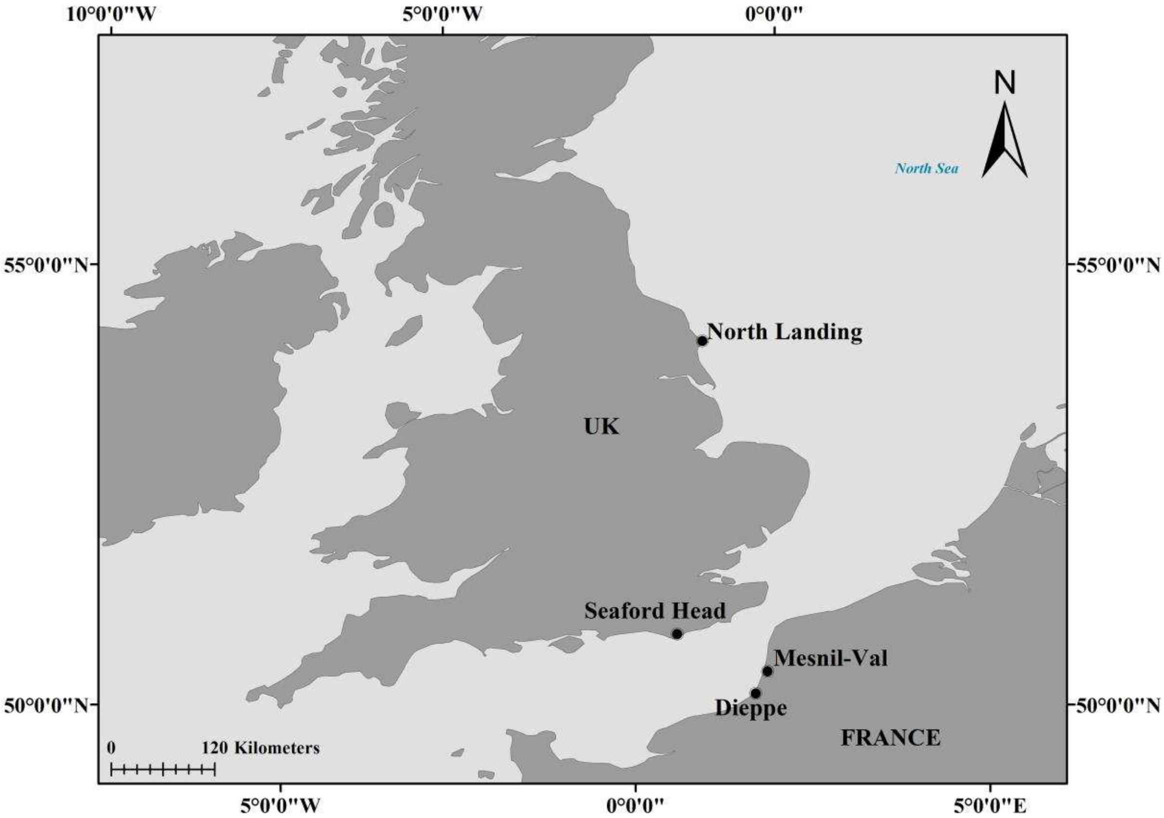
10°0'0"W
5°0'0"W
0°0'0"
N
North Sea
55°0'0"N
55°0'0"N
North Landing
UK
Seaford Head
Mesnil-Val
Dieppe
FRANCE
50°0'0"N
50°0'0"N
0
120 Kilometers
5°0'0"W
0°0'0"
5°0'0"E

Fig. 11

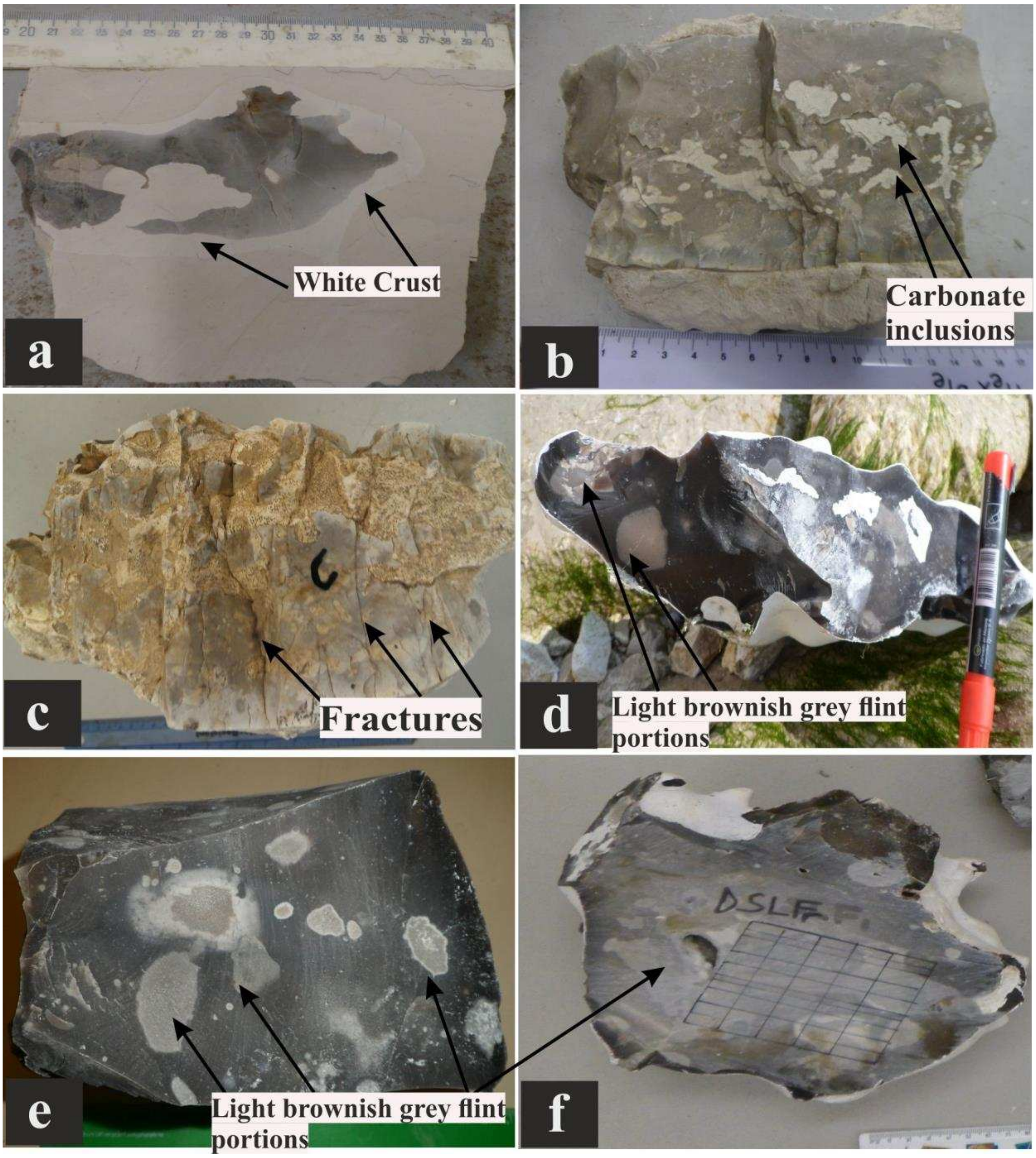
White Crust
a
Carbonate inclusions
b
Fractures
c
Light brownish grey flint portions
d
e
Light brownish grey flint portions
f

Fig. 12

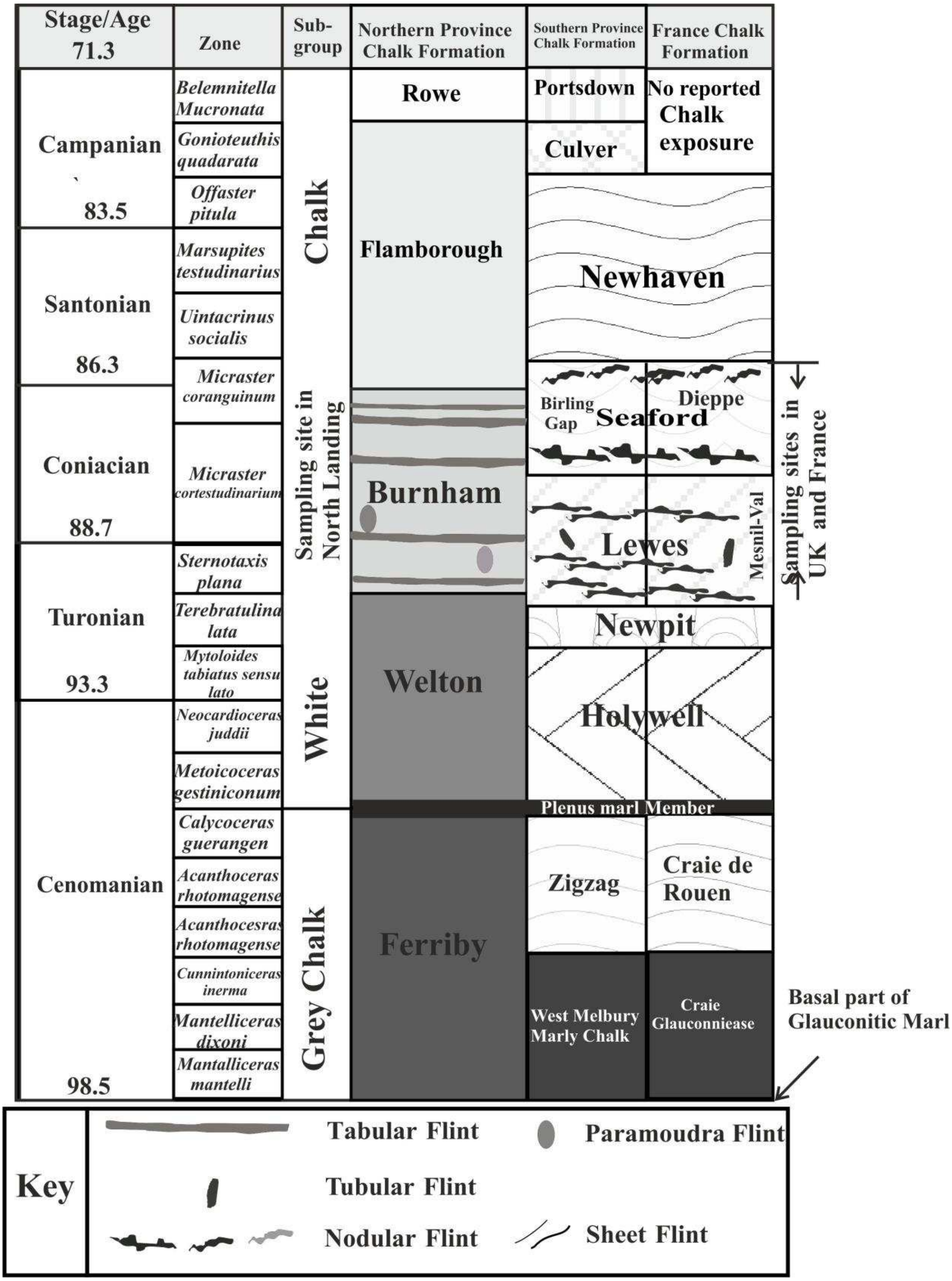

Stage/Age
71.3
Zone
Sub-group
Northern Province Chalk Formation
Southern Province Chalk Formation
France Chalk Formation
Campanian
83.5
Santonian
86.3
Coniacian
88.7
Turonian
93.3
Cenomanian
98.5
Belemnitella Mucronata
Gonioteuthis quadarata
Offaster pitula
Marsupites testudinarius
Uintacrinus socialis
Micraster coranguinum
Micraster cortestudinarium
Sternotaxis plana
Terebratulina lata
Mytoloides tabiatus sensu lato
Neocardioceras juddii
Metoicoceras gestiniconum
Calycoceras guerangen
Acanthoceras rhotomagense
Acanthocesras rhotomagense
Cunnintoniceras inerma
Mantelliceras dixoni
Mantalliceras mantelli
Chalk
White
Grey Chalk
Sampling site in North Landing
Rowe
Flamborough
Burnham
Welton
Ferriby
Portsdown
Culver
No reported Chalk exposure
Newhaven
Birling Gap
Seaford
Dieppe
Lewes
Mesnil-Val
Newpit
Holywell
Plenus marl Member
Zigzag
Craie de Rouen
West Melbury Marly Chalk
Craie Glauconniease
Sampling sites in UK and France
Basal part of Glauconitic Marl
Key
Tabular Flint
Paramoudra Flint
Tubular Flint
Nodular Flint
Sheet Flint

Figure. 13

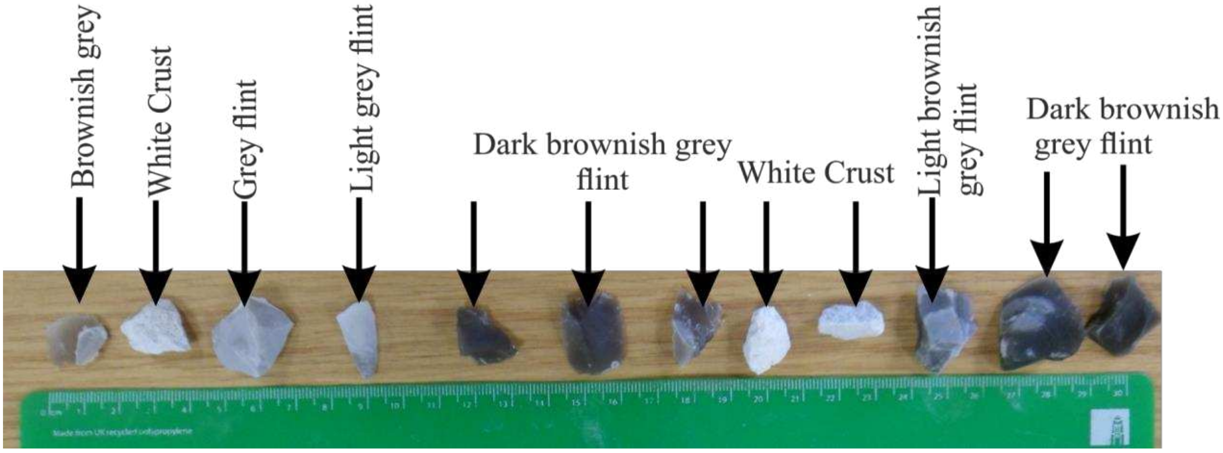
Brownish grey
White Crust
Grey flint
Light grey flint
Dark brownish grey flint
White Crust
Light brownish grey flint
Dark brownish grey flint

Figure 14

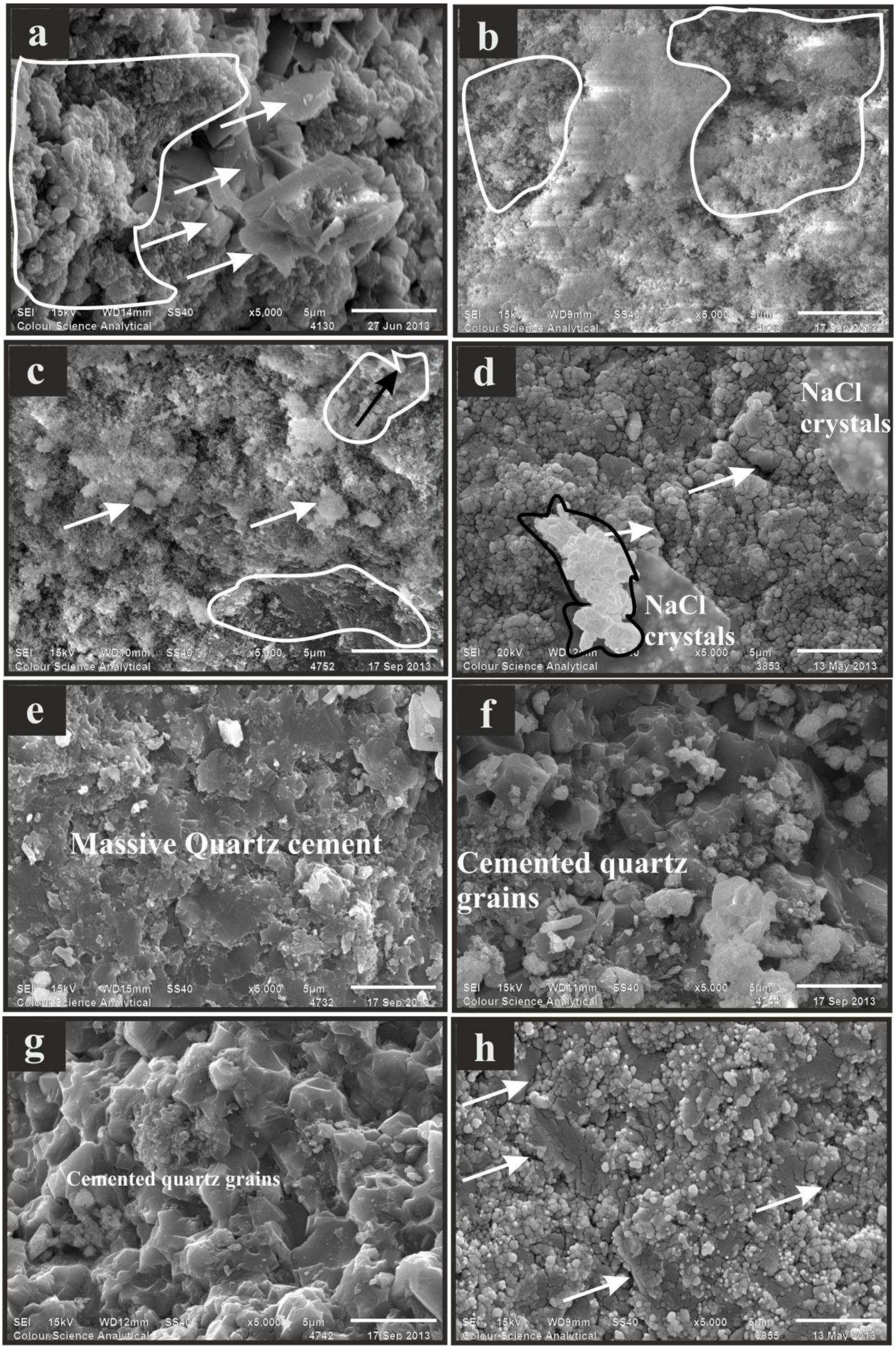
a
SEI 15kV WD14mm SS40 x5,000 5μm
Colour Science Analytical 4130 27 Jun 2013
b
SEI 15kV WD9mm SS40 x5,000 5μm
Colour Science Analytical 17 Sep 2013
c
SEI 15kV WD10mm SS40 x5,000 5μm
Colour Science Analytical 4752 17 Sep 2013
d
NaCl crystals
NaCl crystals
SEI 20kV x5,000 5μm
Colour Science Analytical 3853 13 May 2013
e
Massive Quartz cement
SEI 15kV WD15mm SS40 x5,000 5μm
Colour Science Analytical 4732 17 Sep 2013
f
Cemented quartz grains
SEI 15kV WD11mm SS40 x5,000 5μm
Colour Science Analytical 4744 17 Sep 2013
g
Cemented quartz grains
SEI 15kV WD12mm SS40 x5,000 5μm
Colour Science Analytical 4742 17 Sep 2013
h
SEI 15kV WD9mm SS40 x5,000 5μm
Colour Science Analytical 13 May 2013

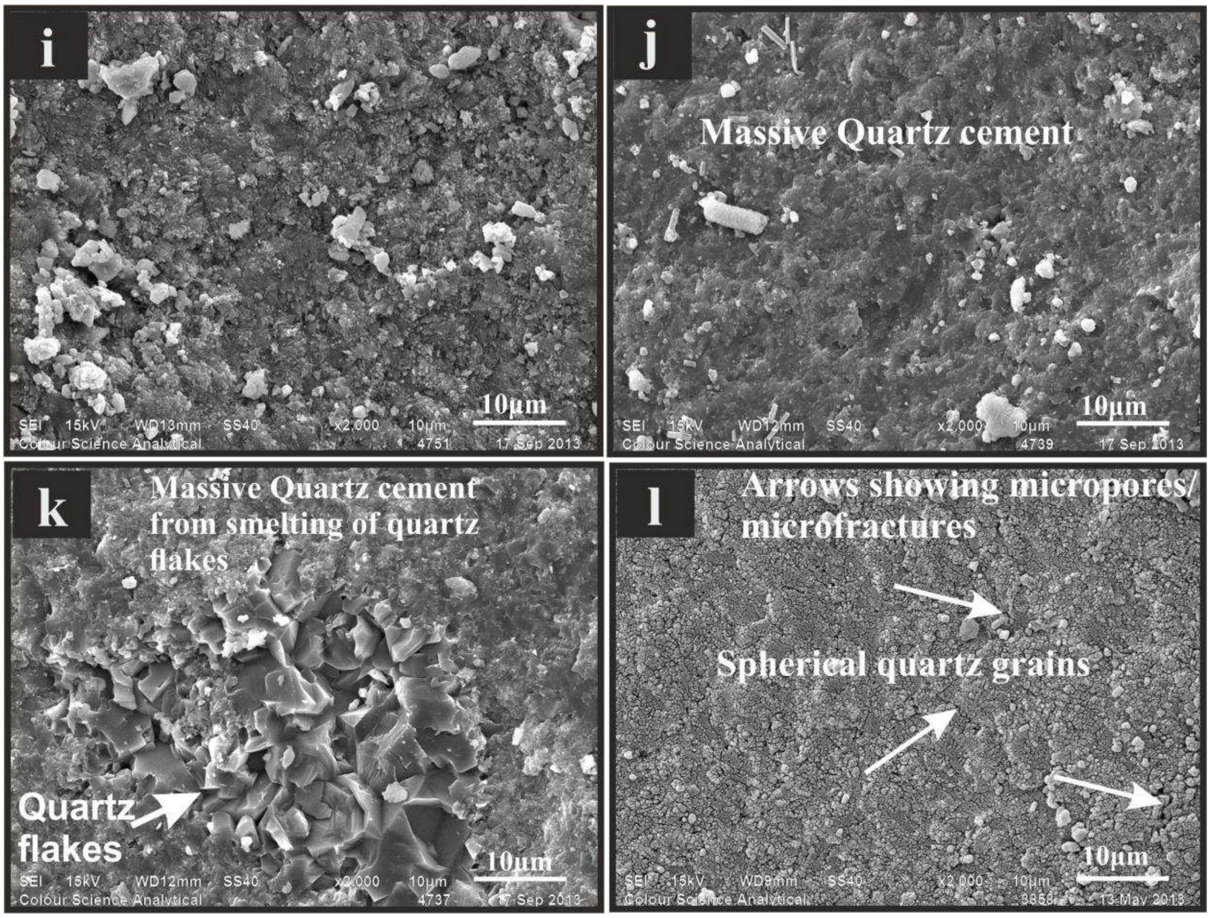

i
j
Massive Quartz cement
k
Massive Quartz cement from smelting of quartz flakes
Quartz flakes
l
Arrows showing micropores/ microfractures
Spherical quartz grains
10µm

Figure 15

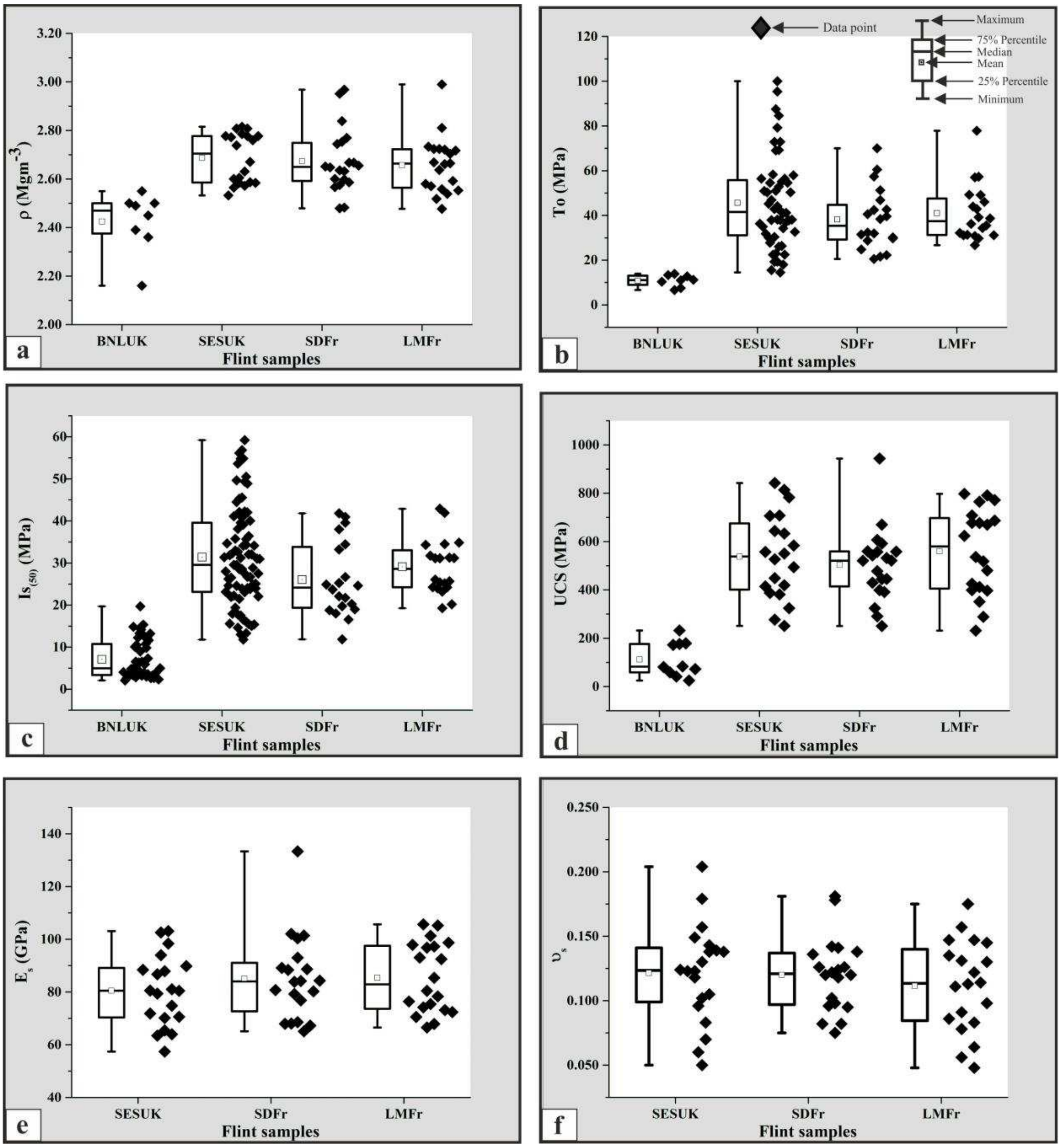
a
ρ (Mgm-3)
Flint samples
BNLUK
SESUK
SDFr
LMFr
b
To (MPa)
Data point
Maximum
75% Percentile
Median
Mean
25% Percentile
Minimum
c
Is(50) (MPa)
d
UCS (MPa)
e
Es (GPa)
f
υs

Figure 16

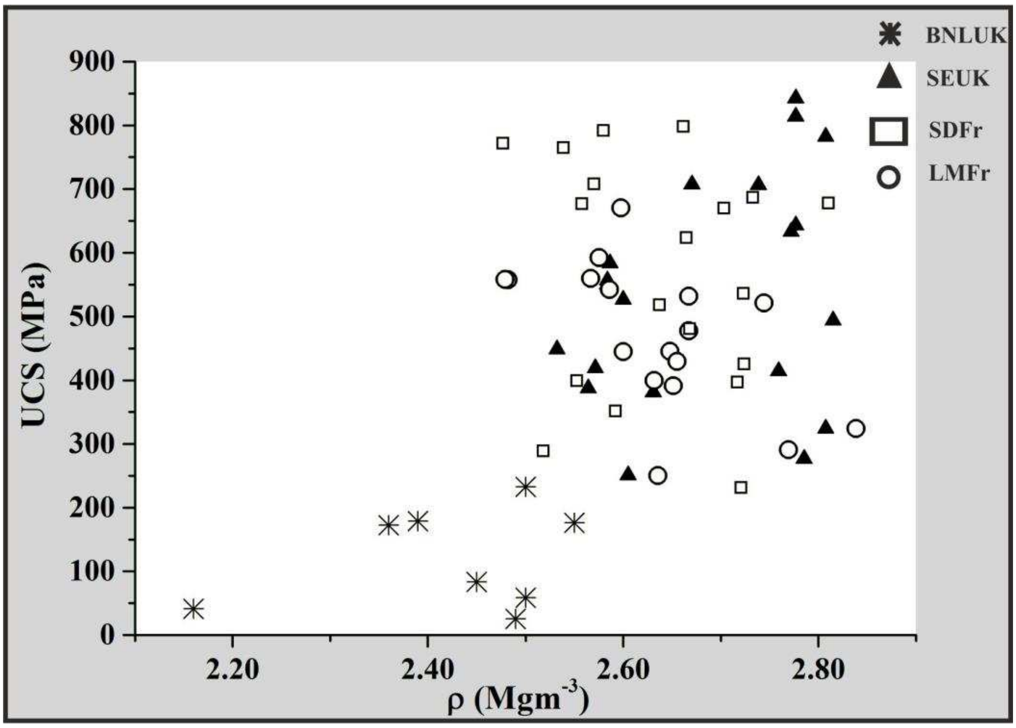

Figure 17

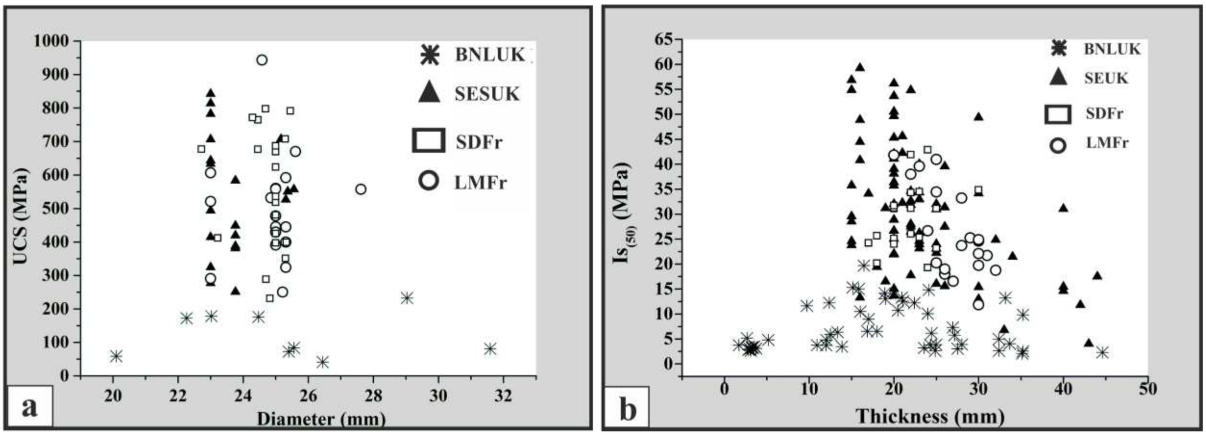

Figure 18

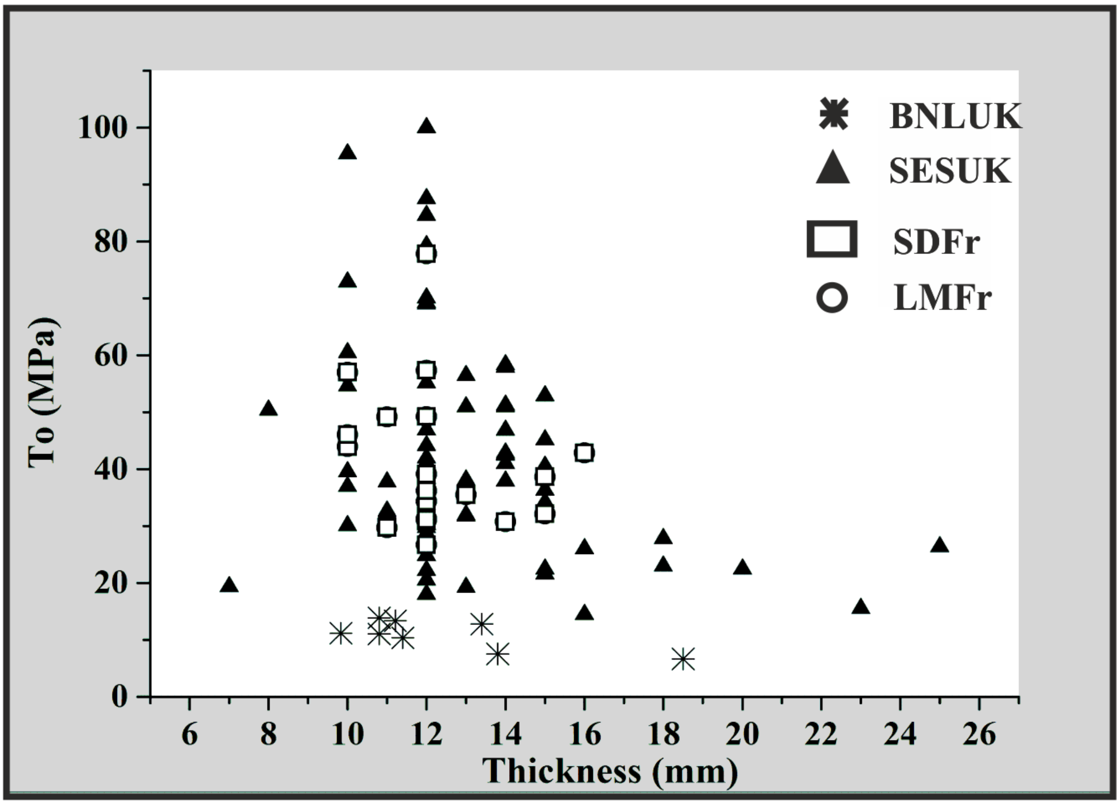

BNLUK
SESUK
SDFr
LMFr
To (MPa)
100
80
60
40
20
0
6
8
10
12
14
16
18
20
22
24
26
Thickness (mm)

Figure 19